

Low-loss GaInNAs saturable absorber mode locking a 1.3- μm solid-state laser

V. Liverini,^{a)} S. Schön, R. Grange, M. Haiml, S. C. Zeller, and U. Keller

Department of Physics, Institute of Quantum Electronics, Swiss Federal Institute of Technology, Zürich, Switzerland

(Received 24 October 2003; accepted 22 March 2004; published online 5 May 2004)

We have demonstrated stable self-starting passive cw mode locking of a solid-state laser at about 1.3 μm using a GaInNAs semiconductor saturable absorber mirror (SESAM). GaInNAs SESAMs show negligible nonsaturable losses, low saturation fluences ($11 \mu\text{J}/\text{cm}^2$) and picosecond decay times which make them well-suited for self-starting and stable cw mode locking. Sub-10-ps pulses were produced with a Nd:YLF laser at 1314 nm. The incorporation of about 2% nitrogen into InGaAs redshifts the absorption edge above 1330 nm and reduces the strain in the saturable absorber grown on a GaAs/AlAs Bragg mirror. Final absorption edge adjustments have been made with thermal annealing which blueshifts the absorption edge. © 2004 American Institute of Physics. [DOI: 10.1063/1.1748841]

Since 1992 it has been demonstrated that semiconductor saturable absorber mirrors (SESAMs)¹⁻³ passive cw mode-lock solid-state lasers without any problems with self-starting and Q-switching instabilities.⁴ The challenge is to grow high-quality SESAMs for longer wavelengths such as 1.3 and 1.5 μm for telecommunication applications. So far, InGaAs quantum wells (QWs) were used for 1.3 μm SESAMs with an indium content of about 40%.⁵ Increasing indium concentration decreases the band gap and therefore redshifts the absorption edge. However, this also increases the lattice mismatch with GaAs giving rise to highly strained layers on GaAs-based Bragg mirrors. High insertion losses due to reduced surface quality and defects are the drawback of this material choice.⁵ InP-based SESAMs and distributed Bragg reflectors (DBRs) would allow for smaller lattice mismatch and therefore less strained InGaAs absorber layers.^{6,7} However, these DBRs have the big disadvantage of small contrast of refractive indices and poor thermal conductivity. The quaternary alloy GaInNAs is a good substitute for InGaAs. QWs with absorption above 1.3 μm can be grown by incorporating just a few percent of nitrogen into InGaAs QWs with lower indium concentration.⁸ Alloying InGaAs with nitrogen also reduces the strain in the QWs, but it decreases the crystalline quality of the layers. For GaInNAs-based active devices, such as vertical-cavity surface-emitting lasers (VCSELs), it is essential to reach good crystalline quality, shown by enhancement of the photoluminescence (PL) signal.⁹ However, for passive devices such as SESAMs, this drawback can be used as an advantage since low photoluminescence intensities are usually associated with faster decay times due to nonradiative recombination. Previously, a GaInNAs SESAM was used to mode-lock a quasi-cw pumped Nd:YLF and Nd:YALO laser at 1.3 μm .¹⁰ No information was given for the saturation fluence of the device and cw mode locking was obtained only with additional active stabilization. In contrast, we demonstrate stable cw mode

locking and provide full SESAM characterization in terms of response time, saturation fluence, modulation depth, and nonsaturable losses.

We have grown both resonant and antiresonant SESAM designs for a more reliable characterization. The resonant GaInNAs SESAM consisted of a 30-pair DBR centered at 1290 nm, a 79-nm-GaAs spacer layer, a 10-nm-GaInNAs saturable absorber layer, and a 10-nm-GaAs cap layer. The antiresonant design was exactly the same except for the cap layer which was 122 nm thick. Figure 1(a) shows the refractive index profile of both SESAMs and the field enhancement in the devices at the operational wavelength of the laser (1314 nm). In Fig. 1(b) the linear reflectivities measured with a CARY 5E photospectrometer are reported. For the resonant SESAM we observed a linear reflectivity of 96.3% and for the antiresonant SESAM of 99.4% at 1314 nm indicating the

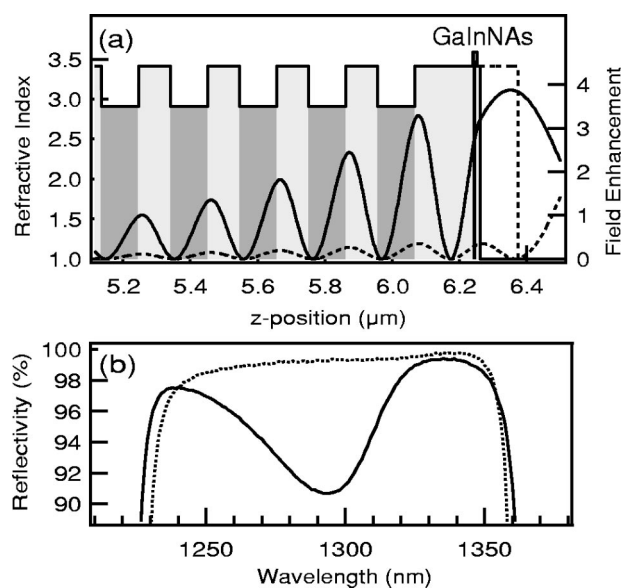


FIG. 1. (a) SESAM design and field intensities; (b) linear reflectivity. Resonant SESAM (solid lines) and antiresonant SESAM (dashed lines). Field intensities are normalized to incident field and calculated for the laser wavelength of 1314 nm.

^{a)}Electronic mail: liverini@phys.ethz.ch

higher modulation depth inherent to resonant designs.

The GaInNAs single quantum wells (SQWs) were grown by molecular beam epitaxy (MBE). A RF nitrogen plasma source was used to produce the nitrogen radicals. Observation of the reflection high-energy electron diffraction (RHEED) during growth showed two-dimensional growth throughout the whole 10-nm-quantum well. Indium and nitrogen concentrations in the SQWs and the layer thicknesses of the SESAMs were determined by high-resolution x-ray rocking curves measurements, which showed extremely good agreement with the desired design. Room temperature PL measurements were used to estimate the band gap. The resonance of the resonant device strongly alters the spectral shape of the PL emission. Therefore, test GaInNAs SQWs with the same characteristics as those grown on the DBRs were grown on GaAs substrates to obtain the PL wavelengths. In contrast, the absorber's band gap can be directly obtained from the antiresonant device when the PL emission is in the stop band of the DBR. By adding about 2% N to $\text{In}_{0.365}\text{Ga}_{0.64}\text{As}$ QWs we were able to obtain photoluminescence at about 1370 nm. Post-growth *ex situ* rapid thermal annealing (RTA) under constant nitrogen flow was essential to tune the PL wavelength closer to the laser wavelength of 1314 nm. In fact, it is well known that GaInNAs QWs blueshift dramatically and improve their crystallinity with annealing temperatures.¹¹ However, we did not want to heal all the defects in order to keep the fast decay times of the devices. By annealing just at 600 °C for 60 s we could blueshift the PL to 1330 nm and still obtain fast recovery times confirmed by optical characterization.

Degenerate pump-probe experiments were performed using 80 MHz, 280 fs pulses from a commercial OPO to observe the time response of the resonant and antiresonant SESAMs. Figure 2(a) shows the normalized time response for the resonant (solid line) and antiresonant (dashed line) devices under the same experimental conditions. Both devices exhibit the same temporal behavior indicating the same defect concentration in the absorber layers. The only evident difference is the lower signal to noise ratio of the antiresonant SESAM due to its much lower modulation depth. Therefore, the resonant device is more suitable for optical characterization. The pump-probe curves show a double exponential decay with a fast 1 ps component, which could be attributed to intraband processes such as thermalization, and a slower 30 ps component. The slow component is ideally suited for self-starting and stable mode locking in the picosecond regime.¹²

Differences between the two designs can otherwise be noticed more clearly in the measurement of their nonlinear reflectivities [Fig. 2(b)], which allow us to obtain the saturation fluence, F_{sat} , the modulation depth, ΔR , and the nonsaturable losses, ΔR_{ns} , of the devices.² The data measured with the 280 fs pulses exhibits a strong rollover due to induced absorption, such as two-photon absorption. It was well fitted with the model function including this induced absorption (solid lines). However, the mode-locked Nd:YLF laser only generated picosecond pulses for which the rollover occurs at much larger fluences as compared to the 280 fs pulses. Therefore, the parameters of the SESAMs were derived from the fit excluding the induced absorption (dotted

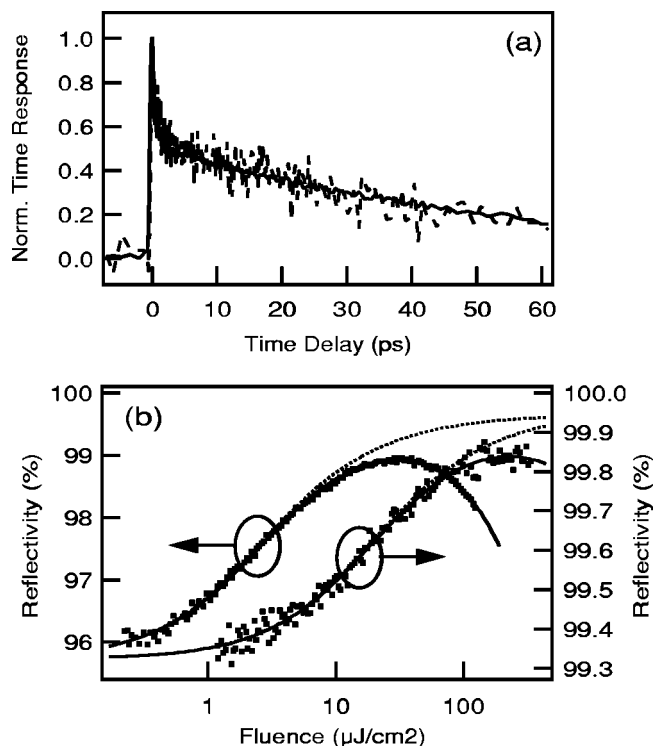


FIG. 2. (a) Normalized time response of the resonant (solid line) and antiresonant (dashed line) SESAMs. Both curves: pump fluence $18 \mu\text{J}/\text{cm}^2$, probe fluence $0.6 \mu\text{J}/\text{cm}^2$; (b) nonlinear reflectivity vs pulse energy fluence of the resonant SESAM (left axis) and the antiresonant SESAM (right axis). Measured data (dots, 280 fs pulses, 1314 nm), fit including induced absorption (solid line), fit without induced absorption for longer pulses (dashed line).

line). We measured a saturation fluence $F_{\text{sat}} = 1 \mu\text{J}/\text{cm}^2$, a modulation depth $\Delta R = 3.9\%$, and nonsaturable losses $\Delta R_{ns} = 0.3\%$ for the resonant design. For the antiresonant design we obtained a saturation fluence $F_{\text{sat}} = 11.2 \mu\text{J}/\text{cm}^2$, a modulation depth $\Delta R = 0.6\%$ and nonsaturable losses $\Delta R_{ns} = 0.04\%$. In comparison, antiresonant InGaAs SESAMs at 1.3 μm were demonstrated with a saturation fluence of several $100 \mu\text{J}/\text{cm}^2$ and much higher nonsaturable losses (up to some percent).⁵ This was most likely due to the reduced surface quality and defects in the highly strained InGaAs layers. Thus, the lower strain resulted in lower nonsaturable losses of only 0.04% for the antiresonant GaInNAs SESAMs compared to InGaAs SESAMs.

As seen in Fig. 1(a), the calculated field enhancement at 1314 nm in the absorber layer of the antiresonant design is 0.29 and in that of the resonant design is 2.5, about 9 times larger. For the same absorber material, the saturation fluence scales inverse linearly and the modulation depth and nonsaturable losses scale linearly with field enhancement. Consequently, we are now able to calculate the saturation fluence of the GaInNAs saturable absorber material itself independent of design influences. Using the results presented above we obtained $3.25 \mu\text{J}/\text{cm}^2$ from the resonant design and $3.75 \mu\text{J}/\text{cm}^2$ from the antiresonant design. We conclude that the saturation fluence of a 10-nm-GaInNAs QW with a PL emission at 1330 nm is $3.5 \pm 0.5 \mu\text{J}/\text{cm}^2$.

To test the performance of the GaInNAs SESAMs we used a Ti:sapphire-pumped Nd:YLF standard delta cavity at 1314 nm with a 1.25% output coupler. Note that the applied

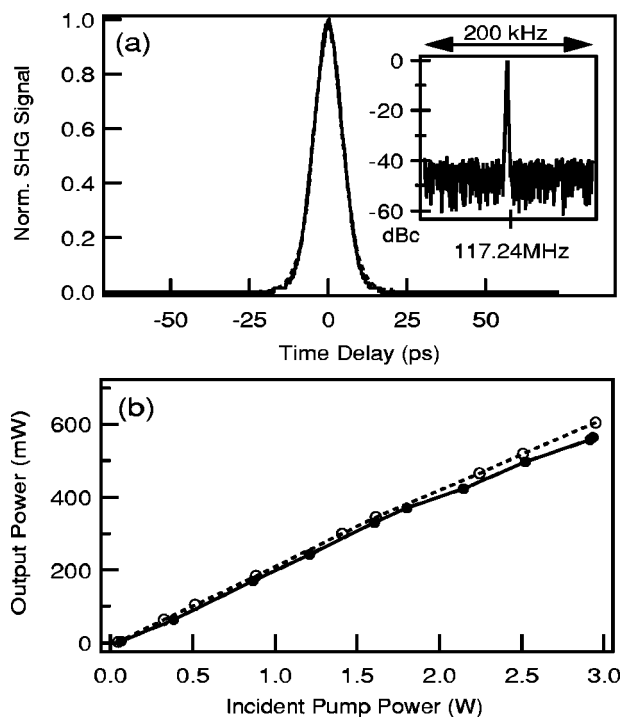


FIG. 3. Laser performance data: (a) intensity autocorrelation of 6.7 ps, data (solid line) and sech²-fit (dashed line). Inset: rf spectrum, logarithmic scale (span: 200 kHz, resolution BW: 1 kHz); (b) output power vs incident pump power with a high reflector (open circles, dashed line) and with the antiresonant SESAM (full circles, solid line).

pumping conditions could also be achieved with diode pumping. Differently from previous experiments of other groups,¹⁰ we demonstrate clean stable self-starting fully passive cw mode locking with our GaInNAs SESAM. A pulse duration as short as 6.7 ps [Fig. 3(a)] fitted with a sech² function at an average output power of 520 mW was measured with the antiresonant SESAM. The pulses had an optical bandwidth of 0.39 nm FWHM giving rise to a time-bandwidth-product of 0.45. The microwave spectrum shown in the inset of Fig. 3(a) clearly demonstrates clean cw mode locking with no sidebands, which would be visible with a spacing of some 10 kHz for Q-switched mode locking (QML). We measured the mode locking buildup time to demonstrate reliable self-starting. When the laser cavity was unblocked, pulsed operation started immediately within 100 μ s with some initial spiking behavior. Stable cw mode locking was reached within 25 ms. The QML threshold was around 490 mW compared to the maximum average output power of 580 mW. A remarkable result is that the average output power was only 10% less than the cw output power obtained replacing the SESAM with a high reflector [Fig. 3(b)]. This is due to the extremely low nonsaturable losses of the SESAM consistent with the nonlinear reflectivity measurements. The shortest pulses and smoothest optical spec-

trum presented here were obtained by flooding the cavity with dry nitrogen to avoid water vapor absorption. We operated the laser for several hours in the cw mode locking regime and no degradation of the SESAM was observed. No difference was noticed in the nonlinear optical parameters and in the mode locking performance within the 5×5 mm² SESAM samples. Moreover, the laser spot could be translated on the SESAM without losing mode locking.

In conclusion, we have demonstrated stable self-starting passive cw mode locking of a solid-state laser at about 1.3 μ m using a GaInNAs SESAM. In contrast with previous attempts,¹⁰ this laser system is free of Q-switching instabilities without the need of active stabilization. The SESAM was based on a standard antiresonant design with a GaInNAs SQW as the saturable absorber and was annealed to shift the PL wavelength to the desired range. Optical characterization showed that the SESAM had very low nonsaturable losses, a low saturation fluence, and a recovery time in the range suitable for self-starting mode locking in the picosecond regime. From our data we could extract the material's saturation fluence of 3.5 ± 0.5 μ J/cm² for the 10-nm-GaInNAs QW close to the band edge. Using our antiresonant GaInNAs SESAM we obtained self-starting stable cw mode locking with 6.7 ps pulses at 1314 nm. The average output power of the laser was very high due to the low nonsaturable losses and the SESAM proved to be robust by working in cw mode-locked operation over several hours at the maximum average output power of 580 mW.

The authors would like to thank M. Golling for the growth of the Bragg mirrors. This work was supported by the National Center of Competence in Research, Quantum Photonics (NCCR-QP) Switzerland and the KTI Project 5781.1 KTS.

- ¹U. Keller, D. A. B. Miller, G. D. Boyd, T. H. Chiu, J. F. Ferguson, and M. T. Asom, *Opt. Lett.* **17**, 505 (1992).
- ²U. Keller, K. J. Weingarten, F. X. Kärtner, D. Kopf, B. Braun, I. D. Jung, R. Fluck, C. Hönninger, N. Matuschek, and J. Aus der Au, *IEEE J. Sel. Top. Quantum Electron.* **2**, 435 (1996).
- ³U. Keller, in *Nonlinear Optics in Semiconductors* Vol 59, edited by E. Garmire and A. Kost (Academic, Boston, 1999), Chap. 4, p. 211.
- ⁴C. Hönninger, R. Paschotta, F. Morier-Genoud, M. Moser, and U. Keller, *J. Opt. Soc. Am. B* **16**, 46 (1999).
- ⁵R. Fluck, G. Zhang, U. Keller, K. J. Weingarten, and M. Moser, *Opt. Lett.* **21**, 1378 (1996).
- ⁶R. Fluck, R. Häring, R. Paschotta, E. Gini, H. Melchior, and U. Keller, *Appl. Phys. Lett.* **72**, 3273 (1998).
- ⁷R. Häring, R. Paschotta, R. Fluck, E. Gini, H. Melchior, and U. Keller, *J. Opt. Soc. Am. B* **18**, 1805 (2001).
- ⁸M. Kondow, K. Uomi, A. Niwa, T. Kitatani, S. Watahiki, and Y. Yazawa, *Jpn. J. Appl. Phys., Part 1* **35**, 1273 (1996).
- ⁹H. Riechert, A. Ramakrishnan, and G. Steinle, *Semicond. Sci. Technol.* **17**, 892 (2002).
- ¹⁰H. D. Sun, G. J. Valentine, R. Macaluso, S. Calvez, D. Burns, M. D. Dawson, T. Joutti, and M. Pessa, *Opt. Lett.* **27**, 2124 (2002).
- ¹¹M. Kondow and T. Kitatani, *Semicond. Sci. Technol.* **17**, 746 (2002).
- ¹²R. Paschotta and U. Keller, *Appl. Phys. B: Lasers Opt.* **73**, 653 (2001).